Original Article
Hydroxycamptothecin-induced apoptotic gene expression profiling by PCR array in human Tenon's capsule fibroblasts

Wei Tang*, Yinong Zhang*, Qing Zhang, Qinghua Wang, Zhifeng Wu

*Department of Ophthalmology, Wuxi No. 2 People's Hospital Affiliated Nanjing Medical University, Wuxi 214002, China. *Equal contributors.*

Abstract: Studies have indicated that hydroxycamptothecin (HCPT) induces apoptosis of fibroblasts. In this study, we investigated the apoptotic gene expression profiling in HCPT-treated -human Tenon's capsule fibroblasts (HTCFs) and identify the most implicated gene in apoptotic signaling of HTCFs by HCPT. Method HTCFs were incubated with HCPT at 0, 0.25 and 4 mg/L for 24, 48 and 72 h, respectively. Anti-proliferative effects were measured by MTT assay. Apoptosis was determined using the Annexin V-FITC/PI apoptosis detection kit and apoptotic cells were identified by flow cytometry. A PCR array was employed to analyze the most implicated apoptotic genes during HCPT-induced apoptosis in HTCFs. Results from our studies showed that HCPT induced apoptosis in HTCFs in a concentration-and time-dependent manner. The apoptotic HTCFs was increased by 9.38% with a multiplicity at 4 mg/L HCPT. PCR array demonstrated remarkable changes in 88 apoptotic genes, including 9 up-regulated genes and 36 down-regulated genes. HCPT treatment induced the upregulation of CHOP and downregulation of XIAP in HTCFs. To conclude, our results support HCPT induced the apoptosis of HTCFs, involving the activation of mitochondrial and endoplasmic reticulum stresses as well as the downregulation expression of XIAP.

Keywords: HCPT, signal pathway, XIAP, HTCFs

Introduction

Glaucoma is a leading cause of bilateral blindness in the world. The glaucoma patients was 60.5 million in 2010, and the estimated number will be increased to 79.6 million by 2020 [1]. Control of intraocular pressure (IOP) is established as the most effective treatment for glaucoma nowadays. Trabeculectomy is widely used to decrease the IOP in cases of glaucoma, although not ideal, the failure rate of trabeculectomy was about 40% after 4 years [2]. The main reason for surgical failure is the proliferation of human Tenon's capsule fibroblasts (HTCFs), which causes scarring in the surgical area. In order to decrease the risk of postoperative scarring, anti-proliferative agents such as mitomycin C or 5-fluorouracil are usually applied to prevent fibroblast growth and scar formation [3, 4]. However, many side effects were accompanied after the administration of anti-proliferative agents, such as chronic hypotony, late-onset bleb leaks, macular degeneration and endophthalmitis [5-7].

Camptothecin (CPT) is a plant alkaloid isolated from the acuminata in southern China. More recently, eukaryotic Topo I has been identified as the cellular target of CPT, which can prevent DNA religation and therefore causes irreversible DNA break during ongoing DNA and RNA synthesis [8, 9]. Hydroxycamptothecin is one of CPT analogues with fewer side effects and is widely used as chemotherapeutic agents for colon cancer, bladder cancer and retinoblastoma [10-12]. Accumulating data have shown that HCPT can induce apoptosis in HTCFs via activating caspase-3 and caspase-9 [13]. However, the underlying mechanisms of HCPT-induced HTCFs apoptosis are still not clear.

The aims of this study are twofold: (1) to investigate the HCPT-induced changes of apoptotic genes of in HTCFs; and (2) to explore the under-
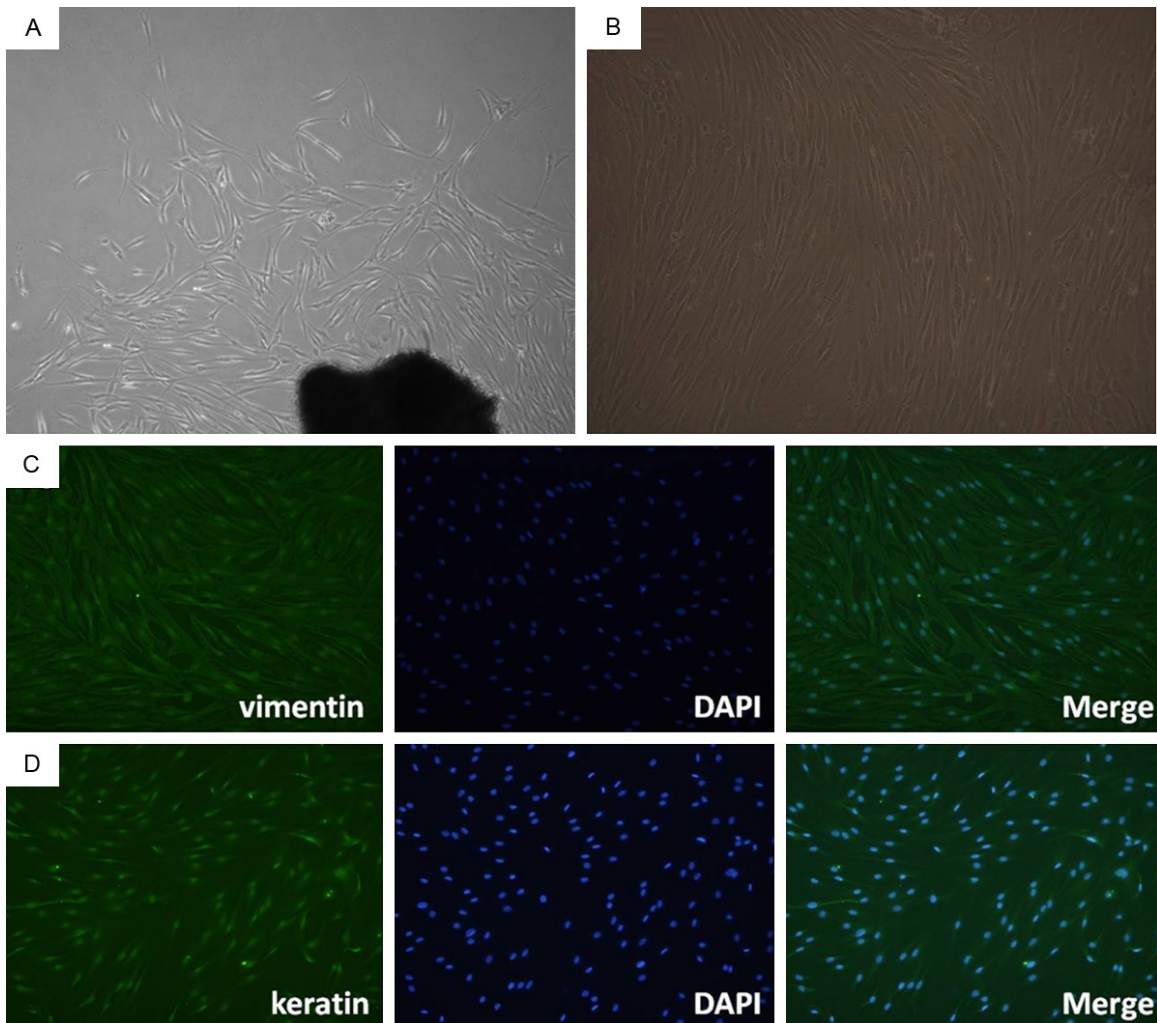
Figure 1. Culture and identification of HTFCs. A. some irregular cells migrated from the initial tissue (100 ×); B. cells showed irregular forms with more abundant cytoplasm and large nuclei after 5-7 d (100 ×); C. immunofluorescene with vimentin-positive staining in green and nuclei (blue) labeled with DAPI (200 ×); D. immunofluorescene with keratin-negative staining and nuclei (blue) labeled with DAPI (200 ×).

lying mechanisms by employing PCR array, a reliable tool for analyzing the expression of focused panel of genes [14].

Materials and methods

Cell culture

HTCFs were isolated from fresh eyes donated to the eye bank of Wuxi No. 2 People's Hospital affiliated Nanjing Medical University. The study conformed to the Declaration of Helsinki, and oral informed consent was obtained from the participants. Cells were maintained in Dulbecco's modified Eagle's medium (DMEM, Gibco, NY) cultured with 10% fetal bovine serum (FBS, Gibco, NY), 0.1 U/L of penicillin and 50 µg/mL streptomycin at 37°C in 5% CO_2

after incubating with HCPT at 0.25 and 4 mg/L, and control (0.9% NaCl only).

Cell proliferation and viability assays

The effects of HCPT on HTCFs proliferation were evaluated by standard MTT assay as previously described [15]. HTCFs were seeded into 96-well plates at an initial density of 6 × 103 cells/well and serum starved overnight. Cells were then incubated in DMEM containing HCPT (0, 0.25 and 0.4 mg/L) for 24, 48 and 72 h, respectively. At the predetermined time point, cultures were washed and incubated in DMEM containing 1 mg/mL MTT. Formazan crystals that formed at 4 h were dissolved in dimethylsulfoxide. Relative concentrations of formazan (as indicators of cell number) were determined
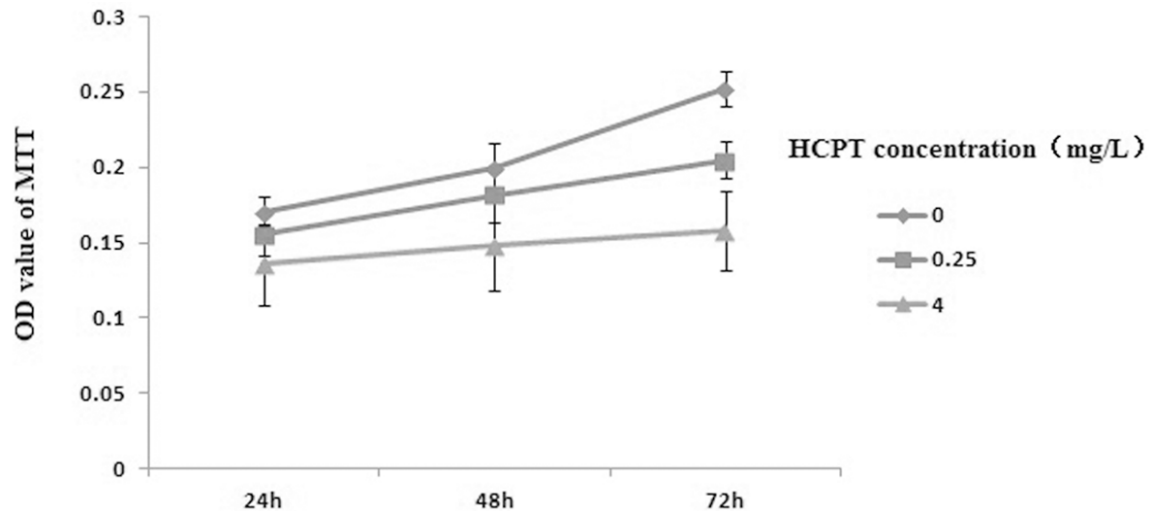
Figure 2. Cell viability of HTCFs measured by MTT. HCPT at the dosage of 0.25 and 4 mg/L caused a significant inhibition of proliferation in HTCFs (Δ means dose-dependent). Differences were significant among 24, 48 and 72 h HCPT groups (*means time-dependent). All experiments were performed at least three times. (*P < 0.05; **P < 0.01).

by quantifying optical absorbance at 490 nm against a control wavelength of 590 nm in an automatic plate reader (Bio-Tek, Elx800, USA). All data were performed in triplicate.

Apoptosis analysis by flow cytometry

Apoptosis assessment was performed by flow cytometry analysis using annexin-V FITC and PI double staining assay as previously described [16]. When HTCFs reached up to 90% confluence, cells were starved for 24 h and treated with 0-4 mg/L HCPT for 24 h. HTCFs were digested with 0.25% trypsin (Gibco, USA), and transferred to 6-well plates. HCPT-treated cells were collected and resuspended at density of 2 × 106 cells/mL in binding buffer containing AnnexinV-FITC and PI, and the mixture were incubated for 10 min in the dark at room temperature. Analysis was immediately performed using Flow Cytometry System (Beckman Coulter, Fullerton, CA).

Real-time PCR array analysis of gene expression profile

Total RNA was isolated using Trizol reagent (Invitrogen, Carlsbad, CA), according to the manufacturer's recommendations RNA of 1 μg was used for reverse transcription using RT kit (CT Bioscience, Cat# CTB101, Changzhou, China) in a 20 μL volume. After reverse transcription, RT products were diluted to 1000 μL

using ddH2O. Mixed the diluted RT products with 1 mL 2 × SYBR Green MasterMix (CT Bioscience, Cat# CTB103, Changzhou, China). Aliquote 20 μL of the mixture to each well of the 96 well PCR array. Load the sealed PCR plate onto Roche LightCycler 480 II. The cycling condition is as follows: 95°C for 5 min in order to activation of hotstart Taq, 95°C for 15 sec, 60°C for 15 sec, 72°C for 20 sec, 45 cycles. Melting curve analysis condition is as follows: 95°C for 5 sec, 65°C for 1 min, 95°C for 0 sec. The house keeping genes: B2M, ACTB, GAPDH, RPL27, HPRT1 and OAZ1 were used to normalize to the amount of RNA. Fold change values were calculated using the formula of 2-ΔΔCt.

PCR array data analysis

The ΔΔCt method was used to perform the relative quantification analysis. ΔΔCt is used to calculate expression fold change. The formula is as follows: 2-ΔΔCt = Target gene expression level of experiment sample/Target gene expression level of control sample.

Statistical analysis

Statistical analysis was carried out using SPSS 13.0 software. Student's t-test was used to analyze differences between groups. For comparisons between multiple groups, one-way ANOVA was followed by SNK tests. Statistical significance was considered at P < 0.05.
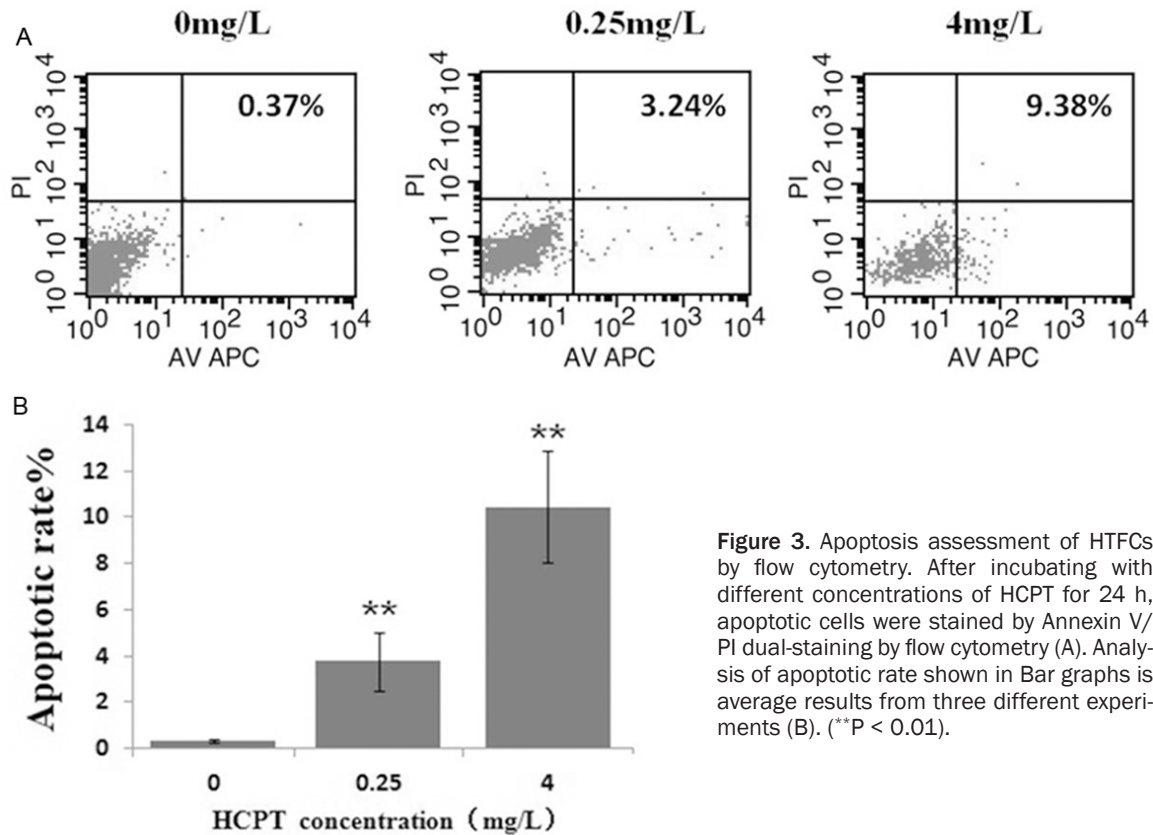
Figure 3. Apoptosis assessment of HTFCs by flow cytometry. After incubating with different concentrations of HCPT for 24 h, apoptotic cells were stained by Annexin V/PI dual-staining by flow cytometry (A). Analysis of apoptotic rate shown in Bar graphs is average results from three different experiments (B). (**P < 0.01).

Results

Culture and identification of HTFCs

The cultured HTFCs were identified as previously describe [13]. After HTFCs adhered to the bottom of the flask, cells gradually migrated from the initial tissue explants (**Figure 1A**). Cells reached up to 90% confluence after 5-7 d (**Figure 1B**). The identification of HTFCs was carried out by immunofluorescence with vimentin and keratin. As shown in **Figure 1C** and **1D**, positive vimentin staining and negative keratin staining indicated that the cultured cells were the HTFCs.

Cell viability assessment by MTT

After incubating with HCPT at the concentration of 0, 0.25 and 4 mg/L for 24, 48 and 72 h, we found an obvious increase in OD values between the 0.25 mg/L HCPT and control groups, while higher concentrations of HCPT inhibited HCTFs proliferation in a dose-dependent manner. Differences were also significant among 24, 48 and 72 h HCPT groups, reflecting a time-dependence manner (P < 0.05). **Figure 2** showed that HCPT exhibited cytotoxic effects on HTCFs, and inhibited cell proliferation of HTCFs in time-and dose-dependent manners.

Apoptosis gene expression

Incubation with HCPT at concentrations of 0, 0.25 and 4 mg/L for 24 h led to apoptotic rates of 0.37%, 3.24% and 9.38% of the cells, respectively (**Figure 3A**). **Figure 3B** showed that the apoptotic rate gradually increased with increasing concentrations of HCPT.

PCR array of 88 apoptotic genes in HTCFs

Among the 88 apoptotic genes, the expression levels of 9 genes [P53, Bax, cytochrome c, caspase-3, caspase-9, IL1A, IL1B, c-fos and C/EBP homologous protein (CHOP)] were up-regulated when compared with the control. Particularly, CHOP was significantly up-regulated. Among 36 down-regulated genes, BCL-2, AKT and XIAP were the most significant (**Table 1**).

HCPT activation of mitochondrial, endoplasmic reticulum and downregulation expression of XIAP in HTCFs

When HTCFs were incubated with HCPT at 4 mg/L for 24 h, the expression levels of Bax,

Table 1. Apoptotic gene expressions with PCR array at 0 and 4 Mg/L HCPT for 24 h

SyMbols	Full naMe (SynonyMs)	HCPT/control (fold changes)
ATF1	Activating transcription factor 1 (EWS-ATF1|FUS/ATF-1|TREB36)	-1.07
ATF2	Activating transcription factor 2 (CRE-BP1|CREB2|HB16|TREB7)	1.37
AIFM1	Apoptosis-inducing factor, Mitochondrion-associated, 1 (AIF|CMTX4)	-2.44
AIFM2	Apoptosis-inducing factor, Mitochondrion-associated, 2 (AMID|PRG3)	-1.28
AKT1	V-akt Murine thyMoMa viral oncogene hoMolog 1 (AKT|CWS6|PKB)	1.32
AKT2	V-akt Murine thyMoMa viral oncogene hoMolog 2 (PKBB|PKBBETA)	-4.65
AKT3	V-akt Murine thyMoMa viral oncogene hoMolog 3 (protein kinase B) (MPPH|PKB-GAMMA|PKBG|PRKBG|RAC-PK-gaMMa|STK-2)	-8.91
APAF1	Apoptotic peptidase activating factor 1 (APAF-1|CED4)	1.01
BID	BH3 interacting doMain death agonist (FP497)	1.07
BCL-2	B-cell CLL/lyMphoMa 2 (Bcl-2|PPP1R50)	-64.71
BCL2L1	BCL2-like 1 (BCL-XL/S|BCL2L|BCLX|bcl-xL|bcl-xS)	-1.17
BAX	BCL2-associated X protein (BCL2L4)	2.63
CASP2	Caspase 2, apoptosis-related cysteine peptidase	-2.21
CASP3	Caspase 3, apoptosis-related cysteine peptidase	7.86
CASP4	Caspase 4, apoptosis-related cysteine peptidase	-1.54
CASP5	Caspase 5, apoptosis-related cysteine peptidase	-1.55
CASP6	Caspase 6, apoptosis-related cysteine peptidase	-1.64
CASP7	Caspase 7, apoptosis-related cysteine peptidase	-1.53
CASP8	Caspase 8, apoptosis-related cysteine peptidase	-3.00
CASP9	Caspase 9, apoptosis-related cysteine peptidase	2.05
CASP10	Caspase 10, apoptosis-related cysteine peptidase	-3.80
CD266	CD226 Molecule (DNAM-1|DNAM1|PTA1|TLiSA1)	-1.72
CD24	CD24 Molecule	-1.34
CD27	CD27 Molecule (S152|T14|TNFRSF7|Tp55)	1.61
CD40LG	CD40 ligand	-1.53
CD5	CD5 Molecule	-2.26
CD70	CD70 Molecule	2.29
CDC2	cyclin-dependent kinase 1	-3.62
DDIT3	DNA-daMage-inducible transcript 3 (CHOP|CHOP-10|CHOP10)	2.01
CYCS	CytochroMe c, soMatic (CYC|HCS|THC4)	7.43
DAPK 1	Death-associated protein kinase 1	-8.20
DAPK 2	Death-associated protein kinase 2	-1.61
FOS	FBJ Murine osteosarcoMa viral oncogene hoMolog (AP-1|C-FOS|p55)	3.93
JUN	Jun proto-oncogene (AP-1|AP1|c-Jun)	1.32
E2F1	E2F transcription factor 1 (E2F-1|RBAP1|RBBP3|RBP3)	-1.24

Apoptotic gene induced by hydroxycamptothecin in fibroblasts

E2F2	E2F transcription factor 2	-2.15
EGFR	EpiderMal growth factor receptor	-10.97
ENDOG	Endonuclease G	1.18
FADD	Activating transcription factor 2	-1.90
FASLG	Fas ligand (TNF superfaMily, MeMber 6)(ALPS1B|APT1LG1|FASL)	-2.28
IFNA2	Interferon, alpha 2	-2.29
IFNB1	Interferon, beta 1, fibroblast	-6.30
IGF1	Insulin-like growth factor 1 (soMatoMedin C)	-12.52
IGF1R	Insulin-like growth factor 1 receptor	-4.22
IKBKB	Inhibitor of kappa light polypeptide gene enhancer in B-cells, kinase beta (IKK-beta|IKK2|IKKB|NFKBIKB)	-1.64
IKBKG	Inhibitor of kappa light polypeptide gene enhancer in B-cells, kinase gaMMa (AMCBX1|FIP-3|FIP3|Fip3p|IKK-gaMMa|IP|IP1|IP2|IPD2|NEMO)	-2.36
IL10	Interleukin 10	1.12
IL1A	Interleukin 1, alpha	3.37
IL1B	Interleukin 1, beta	3.85
IL2	Interleukin 2	-1.97
IL4	Interleukin 4	-3.42
IL6R	Interleukin 6 receptor	1.41
IL7	Interleukin 7	-2.44
IRAK1	Interleukin-1 receptor-associated kinase 1	1.07
JAK2	Janus kinase 2	-5.41
MADD	MAP-kinase activating death doMain	-1.86
MAP3K1	Mitogen-activated protein kinase 1, E3 ubiquitin protein ligase (MAPKKK1|MEKK|MEKK 1|MEKK1|SRXY6)	-3.80
MAP3K5	Mitogen-activated protein kinase 5 (ASK1|MAPKKK5|MEKK5)	-8.55
MAP3K6	Mitogen-activated protein kinase 6 (ASK2|MAPKKK6|MEKK6)	1.25
MAP3K10	Mitogen-activated protein kinase 10 (MEKK10|MLK2|MST)	-2.29
MAP3K11	Mitogen-activated protein kinase 11 (MEKK11|MLK3|PTK1)	-1.71
MAP3K14	Mitogen-activated protein kinase 14	-2.06
MAPK1	Mitogen-activated protein kinase 1 (ERK|ERK2|MAPK2|p38|p40|p41)	-1.89
MAPK3	Mitogen-activated protein kinase 3 (ERK-1|ERK1|ERT2)	-1.53
MAPK8	Mitogen-activated protein kinase 8 (JNK|JNK-46|JNK1|JNK1A2)	-2.60
MAPK9	Mitogen-activated protein kinase 9 (JNK-55|JNK2)	-2.34
MAPK14	Mitogen-activated protein kinase 14 (CSBP|EXIP|Mxi2|SAPK2A|p38)	-2.84
MYD88	Myeloid differentiation priMary response 88	-1.05
NFKB1	Nuclear factor of kappa light polypeptide gene enhancer in B-cells 1 (NF-kB1|NF-kappa-B|NF-kappaB|p105|p50)	1.42
NFKBIA	Nuclear factor of kappa light polypeptide gene enhancer in B-cells inhibitor, alpha (IKBA|MAD-3|NFKBI)	-1.62
NR2C2	Nuclear receptor subfaMily 2, group C, MeMber 2	-2.72
NTRK1	Neurotrophic tyrosine kinase, receptor, type 1	-3.11
PDCD1	PrograMMed cell death 1	-2.84

Apoptotic gene induced by hydroxycamptothecin in fibroblasts

|		
PDCD4	PrograMMed cell death 4 (neoplastic transforMation inhibitor)	-5.72
PDCD7	PrograMMed cell death 7	-1.50
PIK3CA	Phosphatidylinositol-4,5-bisphosphate 3-kinase, catalytic subunit alpha	-2.26
PIK3CG	Phosphatidylinositol-4,5-bisphosphate 3-kinase, catalytic subunit gaMMa	-2.86
PIK3R2	Phosphoinositide-3-kinase, regulatory subunit 2 (beta)(MPPH|P85B|p85)	-1.43
PPP3CC	Protein phosphatase 3, catalytic subunit, gaMMa isozyMe	-2.31
PPP3R1	Protein phosphatase 3, regulatory subunit B, alpha	-1.24
RELA	V-rel reticuloendotheliosis viral oncogene hoMolog A (avian) (NFKB3|p65)	1.42
RIPK1	Receptor (TNFRSF)-interacting serine-threonine kinase 1	-1.63
RPS6KA4	RibosoMal protein S6 kinase, 90kDa, polypeptide 4 (MSK2|RSK-B)	-2.44
RPS6KA5	RibosoMal protein S6 kinase, 90kDa, polypeptide 5 (MSK2|RSK-B)	-2.34
TGFB1	TransforMing growth factor, beta 1 (CED|DPD1|LAP|TGFB|TGFbeta)	-1.13
TNF	TuMor necrosis factor (DIF|TNF-alpha|TNFA|TNFSF2)	1.10
TP53	TuMor protein p53 (BCC7|LFS1|P53|TRP53)	2.23
XIAP	X-linked inhibitor of apoptosis (API3|BIRC4|IAP-3|ILP1|MIHA|XLP2)	-4.98

Negative folds mean down-graduated genes.
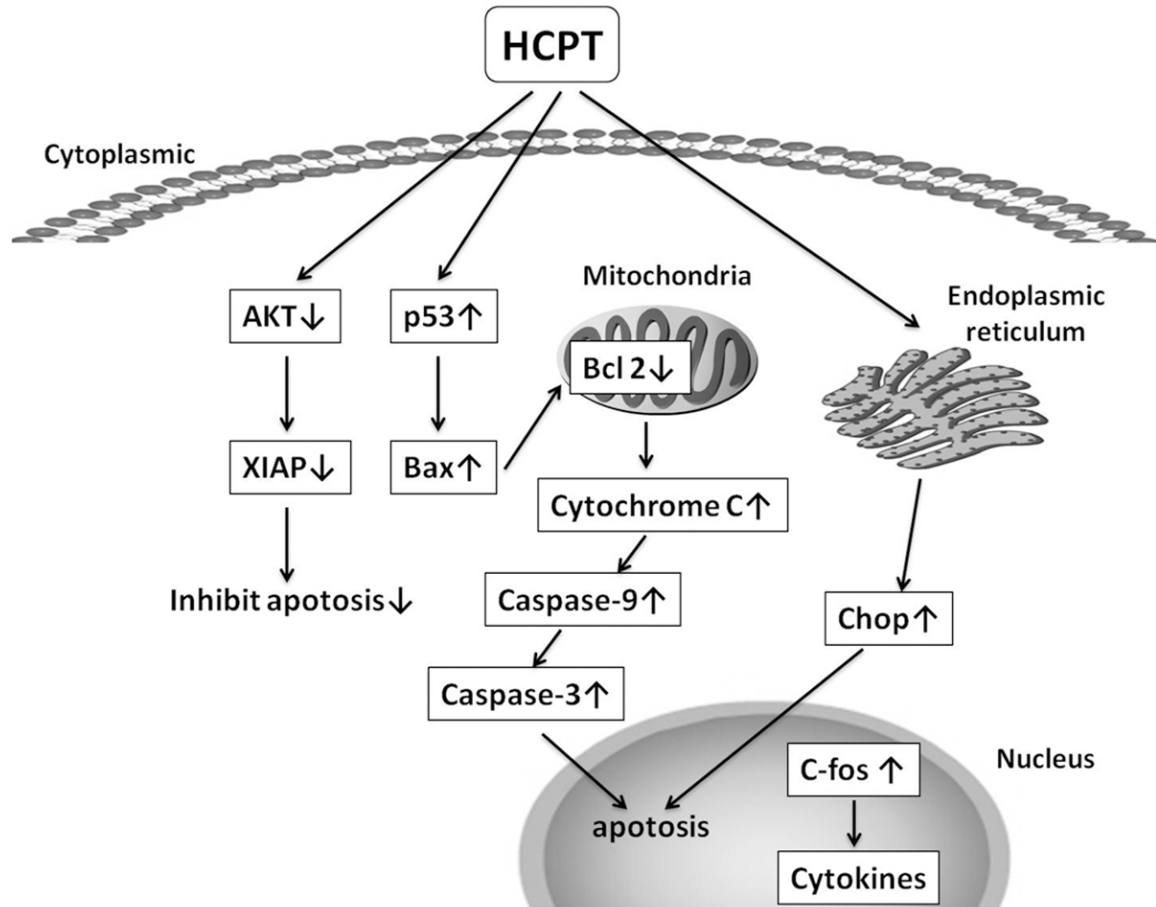
Figure 4. Possible apoptotic signal pathways in HCPT-treated HTFCs. Mitochondrial and endoplasmic reticulum stressed as well as the downregulation expression of XIAP in HTCFs may be involved in the HCPT-induced apoptosis of HTFCs.

P53, cytochrome c, caspase-9, and caspase-3 were promoted by 2.63, 2.23, 7.43, 2.05 and 7.86 fold, respectably. We speculate that HCPT may firstly activate P53 and Bax, and then release cytochrome c to initiate caspase-9, leading to a caspase cascade and apoptosis. We also found that expressions of IL1A, IL1B CHOP and c-fos were increased by 3.37, 3.85, 2.01 and 3.93 fold, respectively, and BCL-2, AKT3 and XIAP were decreased by 64.71, 8.91 and 4.98 fold, respectively. Based on these results and our previous study [13], a possible signal pathway for HCPT induced HTCFs apoptosis was predicted in **Figure 4**.

Discussion

In the current study, we found that different concentrations of HCPT could induce HTCFs apoptosis and inhibit HTCFs proliferation in time- and dose-dependent manners. Nine up-regulated apoptotic genes in HTCFs after HCPT treatment included cytochrome c, IL1A, IL1B, caspase-3, caspase-9, Bax, Chop, c-fos and P53. Thirty-six apoptotic genes were down-regulated, mainly including BCL-2, AKT and XIAP. Our study indicates that the possible apoptotic signal pathways in HCPT-induced HTCFs may be the down-regulation expression of XIAP and activation of mitochondrial and endoplasmic reticulum (ER) stresses.

Apoptosis is a multiple and important biologic process in our lives, which can be divided into intrinsic (mitochondrial) and extrinsic (death receptor) pathways using caspase and caspase-independent pathways [17-19]. The malfunction of mitochondrial can alter the ratio of Bax/Bcl-2 and release of cytochrome c, which will activate the caspase cascade and apoptosis [20, 21]. As we known, Bcl-2 families (anti-apoptotic proteins such as Bcl-2; pro-apoptotic proteins such as Bax) play critical roles in mitochondria apoptosis pathway [22]. In our study,

following the pretreatment of HCPT, the expression levels of Bax, P53, cytochrome c, caspase-9, and caspase-3 in HTCFs were promoted and BCL-2, AKT3 and XIAP were down-regulated. A similar finding was found in the study of Yin who proved that HCPT treatment in HTCFs decreased the expression Bcl-2 and increased expressions of Bax and cytochrome c [23]. The HCPT-induced apoptosis via the mitochondrial-dependent pathway was also found in Sf21 and I OZCAS-Spex-II cell lines [24]. In addition, our previous study confirmed that the protein levels of cleavage caspase -3 (17KD), caspase-3 and caspase-9 were up-regulated in HTCFs after treatment with HCPT [13]. All these above-mentioned findings suggested mitochondria may play an important role in regulating HCPT-induced apoptosis in HTCFs.

ER stress is also one of apoptotic pathways in cells, which can be triggered by many physiological and pathophysiological conditions [25, 26]. The transcription factor CHOP can mediate apoptosis by triggering the ER stress [27, 28]. Our findings showed that HCPT promoted the expression levels of CHOP and Bax, and decreased the expression of Bcl-2, which implied that HCPT-induced apoptosis of HTCFs may be via ER in HTCFs. The activation of caspases is considered to be irreversible, but this activation process can be blocked by some proteins such as the Inhibitor of Apoptosis Proteins (IAPs). The expression of IAPs has been confirmed in many species and XIAP is the best characterized member in IAP proteins [29]. Some researchers found that XIAP was the only IAP that could directly bind and inhibit caspases by preventing caspase-9 monomers and interfering with dimerization-based caspase-9 activation [30-32]. It has been reported that HCPT induced apoptosis and inhibited tumor growth in colon cancer by down-regulating the expression of XIAP [10]. In this study, we found HCPT down-regulated expressions of XIAP and AKT3, activated caspase-9 and caspase-3, and finally induced apoptosis of HTCFs, which may be related to the apoptosis inhibition of HTCFs. Our results provide the theoretical evidence that HCPT-induced degradation of XIAP and AKT may bean impartment contributor to HCPT-induced apoptosis.

Proliferation of HTCFs after trabeculectomy has always been a burning question and the inhibition of HTCFs proliferation is regarded as the key step to reduce the surgical failure rate HCPT, as a new anti-proliferative agent, not only brings hope to improve the surgical success rate in trabeculectomy but also proposes more possibilities in decreasing the risks of proliferative vitreoretinopathy in retinal disease and recurrent pterygium, and inducing apoptosis of lens epithelial cells in posterior capsular opacification and human retinoblastoma cells in retinoblastoma [12].

In conclusion, our current study demonstrates that HCPT induced cell apoptosis and inhibited cell growth in HTCFs via down-regulating the expression of XIAP and activating the mitochondrial and endoplasmic reticulum stress. The exact mechanism of intracellular signal transduction remains to be determined, but our current study indicates that HCPT as a new anti-proliferative agent may be applied to prevent fibroblast growth and scar formation during trabeculectomy.

Acknowledgements

Disclosure of conflict of interest

None.

Address correspondence to: Dr. Zhifeng Wu, Wuxi Second People's Hospital Affiliated with Nanjing Medical University, Wuxi 214002, China. Tel: 86 510 66681222; Fax: 86 510 82754933; E-mail: zhifengwu@hotmail.com

References

[1] Quigley HA, Broman AT. The number of people with glaucoma worldwide in 2010 and 2020. Br J Ophthalmol 2006; 90: 262-7.

[2] Jampel HD, Solus JF, Tracey PA, Gilbert DL, Loyd TL, Jefferys JL, Quigley HA. Outcomes and bleb-related complications of trabeculectomy. Ophthalmology 2012; 119: 712-722.

[3] Wilkins M, Indar A, Wormald R. Intra-operative mitomycin C for glaucoma surgery. Cochrane Database Syst Rev 2005; 4: CD002897.

[4] Eşme A, Yildirim C, Tatlipinar S, Düzcan E, Yaylali V, Ozden S. Effects of intraoperative sponge mitomycin C and 5-fluorouracil on scar formation following strabismus surgery in rabbits. Strabismus 2004; 12: 141-8.

[5] Yoon PS, Singh K. Update on antifibrotic use in glaucoma surgery, including use in trabeculectomy and glaucoma drainage implants and combined cataract and glaucoma surgery. Curr Opin Ophthalmol 2004; 15: 141-6.

[6] Palanca-Capistrano AM, Hall J, Cantor LB, Morgan L, Hoop J, WuDunn D. Long-term outcomes of intraoperative 5-fluorouracil versus intraoperative mitomycin C in primary trabeculectomy surgery. Ophthalmology 200; 116: 185-90.

[7] Rodrigues AM, Júnior AP, Montezano FT, de Arruda Melo PA, Prata J Jr. Comparison between results of trabeculectomy in primary congenital glaucoma with and without the use of mitomycin C. J Glaucoma 2004; 13: 228-32.

[8] Gupta D, Bronstein IB, Holden JA. Expression of DNA topoisomerase I in neoplasms of the kidney: correlation with histological grade, proliferation, and patient survival. Hum Pathol 2000; 31: 214-219.

[9] Pommier Y. Topoisomerase I inhibitors: camptothecins and beyond. Nat Rev Cancer 2006; 6: 789-802.

[10] Fei B, Chi AL, Weng Y. Hydroxycamptothecin induces apoptosis and inhibits tumor growth in colon cancer by the downregulation ofsurvivin and XIAP expression. World J Surg Oncol 2013; 11: 120.

[11] Wang Y, Wang H, Zhang W, Shao C, Xu P, Shi CH, Shi JG, Li YM, Fu Q, Xue W, Lei YH, Gao JY, Wang JY, Gao XP, Li JQ, Yuan JL, Zhang YT. Genistein sensitizes bladder cancer cells to HCPT treatment in vitro and in vivo via ATM/NF-κB/IKK pathway-induced apoptosis. PLoS One 2013; 8: e50175.

[12] Han S, Wei W. Camptothecin induces apoptosis of human retinoblastoma cells via activation of FOXO1. Curr Eye Res 2011; 36: 71-7.

[13] Tang W, Zhang Y, Qian C, Yuan Z, Du J. Induction and Mechanism of Apoptosis by Hydroxycamptothecin in Human Tenon's Capsule Fibroblasts. Invest Ophthalmol Vis Sci 2012; 53: 4874-80.

[14] Zheng M, Lv LL, Cao YH, Liu H, Ni J, Dai HY, Liu D, Lei XD, Liu BC. A pilot trial assessing urinary gene expression profiling with an mRNA array for diabetic nephropathy. PLoS One 2012; 7 e34824.

[15] Yu YL, Yu SL, Su KJ, Wei CW, Jian MH, Lin PC, Tseng IH, Lin CC, Su CC, Chan DC, Lin SZ, Harn HJ, Chen YL. Extended O6-methylguanine methyltransferase promoter hypermethylation following n-butylidenephthalide combined with 1,3-bis(2-chloroethyl)-1-nitrosourea (BCNU) on inhibition of human hepatocellular carcinoma cell growth. J Agric Food Chem 2010; 58: 1630-8.

[16] Ying TH, Yang SF, Tsai SJ, Hsieh SC, Huang YC, Bau DT, Hsieh YH. Fisetin induces apoptosis in human cervical cancer HeLa cells through

ERK1/2-mediated activation of caspase-8-/caspase-3-dependent pathway. Arch Toxicol 2012; 86: 263-73.

[17] Sheridan JP, Marsters SA, Pitti RM, Gurney A, Skubatch M, Baldwin D, Ramakrishnan L, Gray CL, Baker K, Wood WI, Goddard AD, Godowski P, Ashkenazi A. Control of TRAIL-induced apoptosis by a family of signaling and decoy receptors. Science 1997; 277: 818-21.

[18] Huang SH, Wu LW, Huang AC, Yu CC, Lien JC, Huang YP, Yang JS, Yang JH, Hsiao YP, Wood WG, Yu CS, Chung JG. Benzyl isothiocyanate (BITC) induces G2/M phase arrest and apoptosis in human melanoma A375.S2 cells throughreactive oxygen species (ROS) and both mitochondria-dependent and death receptor-mediated multiplesignaling pathways. J Agric Food Chem 2012; 60: 665-675.

[19] Yang JH, Chou CC, Cheng YW, Sheen LY, Chou MC, Yu HS, Wei YH, Chung JG. Effects of glycolic acid on the induction of apoptosis via caspase-3 activation in human leukemia cell line (HL-60). Food Chem Toxicol 2004; 42: 1777-1784.

[20] Lu TH, Su CC, Chen YW, Yang CY, Wu CC, Hung DZ, Chen CH, Cheng PW, Liu SH, Huang CF. Arsenic induces pancreatic β-cell apoptosis via the oxidative stress-regulated mitochondria-dependent and endoplasmic reticulum stress-triggered signaling pathways. Toxicol Lett 2011; 201: 15-26.

[21] Khanbolooki S, Nawrocki ST, Arumugam T, Andtbacka R, Pino MS, Kurzrock R, Logsdon CD, Abbruzzese JL, McConkey DJ. Nuclear factor-kappaB maintains TRAIL resistance in human pancreatic cancer cells. Mol Cancer Ther 2006; 5: 2251-60.

[22] Burlacu A. Regulation of apoptosis by Bcl-2 family proteins. J Cell Mol Med 2003; 7: 249-57.

[23] Yin X, Sun H, Yu D, Liang Y, Yuan Z, Ge Y. Hydroxycamptothecin induces apoptosis of human tenon's capsule fibroblasts by activating the PERK signaling pathway. Invest Ophthalmol Vis Sci 2013; 54: 4749-58.

[24] Zhang L, Zhang Y, He W, Ma D, Jiang H. Effects of camptothecin and hydroxycamptothecin on insect cell lines Sf21 and IOZCAS-Spex-II. Pest Manag Sci 2012; 68: 652-7.

[25] Asada R, Kanemoto S, Kondo S, Saito A, Imaizumi K. The signalling from endoplasmic reticulum-resident bZIP transcription factors involved in diverse cellular physiology. J Biochem 2011; 149: 507-18.

[26] Szegezdi E, Macdonald DC, Ní Chonghaile T, Gupta S, Samali A. Bcl-2 family on guard at the ER. Am J Physiol Cell Physiol 2009; 296: C941-53.

[27] Kim I, Xu W, Reed JC. Cell death and endoplasmic reticulum stress: disease relevance and

therapeutic opportunities. Nat Rev Drug Discov 2008; 7: 1013-30.

[28] Oyadomari S, Mori M. Roles of CHOP/ GADD153 in endoplasmic reticulum stress. Cell Death Differ. 2004; 11: 381-9.

[29] Salvesen GS, Duckett CS. IAP proteins: blocking the road to death's door. Nat Rev Mol Cell Biol 2002; 3: 401-10.

[30] Salvesen GS, Abrams JM. Caspase activation-stepping on the gas or releasing the brakes? Lessons from humans and flies. Oncogene 2004; 23: 2774-84.

[31] Eckelman BP, Salvesen GS. The human anti-apoptotic proteins cIAP1 and cIAP2 bind but do not inhibit caspases. J Biol Chem 2006; 281: 3254-60.

[32] Shiozaki EN, Chai J, Rigotti DJ, Riedl SJ, Li P, Srinivasula SM, Alnemri ES, Fairman R, Shi Y. Mechanism of XIAP-mediated inhibition of caspase-9. Mol Cell 2003; 11: 519-27.